ELSEVIER

International Journal of Pharmaceutics 108 (1994) 21–29

international journal of pharmaceutics

Pharmacokinetics and tissue distribution of methotrexate after intravenous injection of differently charged liposome-entrapped methotrexate to rats

Chong-Kook Kim *, Mi-Kyung Lee, Jeong-Hee Han, Beom-Jin Lee

College of Pharmacy, Seoul National University, San 56-1, Shinlim-Dong, Kwanak-Gu, Seoul 151-742, South Korea

(Received 31 August 1993; Modified version received 6 December 1993; Accepted 17 December 1993)

Abstract

Liposome-entrapped [^{3}H]MTX was prepared by modification of reverse-phase evaporation vesicle (REV) methods. Neutral liposomes were prepared with a mixture of phosphatidylcholine (PC), cholesterol (CH) and α-tocopherol (α-T) (8:4:0.1, molar ratio). Positively and negatively charged liposomes were also prepared by incorporation of stearylamine (SA) (8:4:0.1:1, molar ratio) and dicetyl phosphate (DCP) (8:4:0.1:1, molar ratio) into neutral liposomes, respectively. The release profiles of [^{3}H]MTX from liposomes in the presence of rat plasma were the same shape regardless of surface charges, showing initial fast release followed by much slower release. The release profiles of [^{3}H]MTX from liposomes were dependent on the surface charge of liposomes. Negatively charged liposomes showed much greater [^{3}H]MTX release compared to positively charged and neutral liposomes. The enhanced in vitro release of [^{3}H]MTX from negatively charged liposomes in the presence of rat plasma may be due to the interaction of incorporated lipid compositions of liposomes with plasma components, resulting in a change in drug release through the lipid bilayers by destabilization of the liposomal membranes. After intravenous (i.v.) injection of free and liposome-entrapped [^{3}H]MTX to rats, the elimination of [^{3}H]MTX from the blood stream showed biphasic patterns indicating rapid declining disposition up to 30 min followed by a slower elimination phase. Liposome-entrapped [^{3}H]MTX maintained a higher and longer plasma concentration, and mainly intact form in plasma compared to free [^{3}H]MTX for 2 h. Liposome-entrapped [^{3}H]MTX enhanced bioavailability in plasma due to the retardation of drug release and protection of drug clearance by lipid bilayers of liposomes. Negatively charged liposome-entrapped drug was cleared more rapidly from the blood, resulting from the rapid uptake by liver to a greater extent, possibly via the reticuloendothelial system (RES), since liposome-entrapped drug cannot be eliminated by the kidney, the main eliminating organ for MTX. The tissue distribution of liposome-entrapped [^{3}H]MTX was widely different when compared to free [^{3}H]MTX. There was a markedly increased uptake of drug in spleen from neutral and negatively charged liposomes. Negatively charged liposomes also increased localization of drug in liver, lung and lymph nodes compared to neutral and positively charged liposomes at 2 h after i.v. injection to rats. From these findings, liposomes containing anticancer drugs would appear to be an effective carrier system for targeting to these sites. Although liposome-entrapped [^{3}H]MTX was widely distributed in tissues without the exact role of the liposomal surface charge being known, it was evident that the surface charge of liposomes altered the biodistribution and membrane permeation of drug.

* Corresponding author.

SSDI 0378-5173(94)00007-R

Key words: Methotrexate; Liposome-entrapped methotrexate; Gel chromatography; Charged liposomes; Pharmacokinetics; Tissue distribution

1. Introduction

In chemotherapy, chemotherapeutic agents must be delivered to target sites in appropriate amounts over a long period without toxicity to normal tissues. Liposomes have some advantages over other carriers by virtue of being nontoxic, biodegradable, biocompatible and having low antigenicity (Kim et al., 1991; Kim et al., 1993a,b; Bae et al., 1993). Liposome entrapping anticancer agents provide the possibility of selective drug delivery and reducing systemic cytotoxicity due to their carrier properties (Juliano et al., 1978; Rahman et al., 1978). The disposition and localization of liposome-entrapped drug are known to be affected by various factors such as the route of administration, particle size, surface charge and lipid compositions (Jonah et al., 1975; Juliano and Stamp, 1975; Kirby et al., 1980; Hirano and Hunt, 1985; Sada et al., 1990). The effects of surface charge and lipid composition on the disposition and in vivo behavior of liposome-encapsulated drugs have been widely investigated.

Methotrexate (MTX), a folic acid antagonist, has widely been used in chemotherapy to treat various types of neoplastic diseases such as osteosarcoma, choriosarcoma, head-and-neck and breast cancer (Bleyer, 1978). MTX exerts its cytotoxic activity by competitively inhibiting dihydrofolate reductase, the intracellular enzyme responsible for converting folic acid to folate cofactors (Shen and Azarnoff, 1978). The effect of surface charge and lipid compositions on the pharmacokinetics and tissue dispostion of MTX were previously investigated (Kimelberg et al., 1976; Kimelberg and Atchison, 1978; Kim et al., 1993a; Bae et al., 1993). Positively charged liposomes containing MTX enhance chemotherapeutic efficacy against solid rodent tumors and resistant human leukemic cell lines due to their association with tumor cells compared to free MTX (Kosloski et al., 1978). MTX entrapped in positively and negatively charged liposomes produces markedly increased uptake into spleen and liver (Colley and Ryman, 1975; Kimelberg et al., 1976). However, the effects of liposomal surface charge and lipid compositions on the pharmacokinetics and tissue disposition of anticancer drugs are still a matter of debate.

The purpose of this research was to investigate extensively the pharmacokinetics and tissue distribution of [^{3}H]MTX after i.v. injection of free [^{3}H]MTX and liposome-entrapped [^{3}H]MTX to rats for varying lipid compositions and surface charge of liposomes. [^{3}H]MTX was used as a radioactive tracer drug.

2. Materials and methods

2.1. Materials

Egg phosphatidylcholine (PC), α-tocopherol (α-T), stearylamine (SA), dicetyl phosphate (DCP) and cholesterol (CH) were purchased from Sigma Chemical Co. (St. Louis, MO, U.S.A.). Unlabeled methotrexate (MTX) was kindly supplied courtesy of Choong Wae Pharmaceutical Co. (Seoul, South Korea). Sodium salt of tritium-labeled [^{3}H]MTX was a product of Amersham International (Buckinghamshire, U.K.). The stock solution of [^{3}H]MTX in distilled water was used without further purification. Soluene-350® (0.5 N quartenary ammonium in toluene; $C_{25}H_{55}NO$) was purchased from Packard Instrument Co. (Downers Grove, IL, U.S.A.). 2,5-Diphenyloxazole (PPO) and 1,4-[2-(5-phenyloxazolyl)]benzene (POPOP) for the preparation of scintillation cocktail were products of Sigma Chemical Co.(St. Louis, MO, U.S.A.). Triton X-100 was provided by Duksan Pharmaceutical Co. (Seoul, South Korea). Sephadex G-50 was obtained from Pharmacia Fine Chemicals (Piscataway, NJ, U.S.A.). Dialysis bag (Mol. Wt range, 12000–14000, diameter 15.9 mm) was obtained from Medicell International LTD (London, U.K.). All other chemicals were of reagent grade and used without futher purification.

2.2. Preparation of liposomes

Liposome-entrapped [^{3}H]MTX was prepared by modification of reverse-phase evaporation vesicle (REV) methods as reported previously (Szoka and Papahadjopoulous, 1978). Neutral liposomes were prepared with a mixture of PC, CH and α-T (8:4:0.1, molar ratio). Positively and negatively charged liposomes were also prepared by incorporation of SA (8:4:0.1:1, molar ratio) and DCP (8:4:0.1:1, molar ratio) into neutral liposomes, respectively. A total of 40 μmol of lipids was dissolved in chloroform and evaporated to dryness on a rotary evaporator. The dried thin lipid film was then redissolved in a mixture of chloroform (1 ml) and isopropyl ether (2 ml). 1 ml of phosphate-buffered saline (PBS, pH 7.4) containing 250 μg of unlabeled MTX and 5 μCi of [^{3}H]MTX as a tracer was added. The resulting binary mixtures were then mechanically shaken using a vortex-type mixer for 1 min followed by 30 s incubation. Organic solvent was removed under reduced pressure (360 mmHg) at 20–25°C. As the solvent was removed, a homogeneous opalescent viscous gel was formed. At this point, an appropriate amount of PBS was added and the suspension was placed on the rotary evaporator to further remove traces of solvents for an additional 15 min at 20°C. The newly formed liposomes were allowed to anneal at room temperature for 30 min followed by rapid cooling. All liposomal prerarations were stored at 4°C and used within 12 h. The liposomes prepared as mentioned above were known to be stable at least for 7 days at 4°C (Kim et al., 1991, 1993b).

2.3. Determination of encapsulation efficiency

Liposomal suspension was ultracentrifuged at 45000 rpm (180000 $\times g$) for 15 min. The supernatant was carefully collected using a pasteur pipette. The pelleted vesicles were resuspended in PBS and washing repeated twice. The final pellets were resuspended in PBS of appropriate dilution. A liposomal aliquot (50 μl) was withdrawn and the radioactivity of [^{3}H]MTX entrapped in liposomes was counted using a liquid scintillation counter (Raca Beta, LKB Wallac Co., Turku, Finland).

2.4. In vitro release studies

In vitro release of liposome-entrapped [^{3}H]-MTX was studied according to a dialysis method reported previously (Mayhew et al., 1984). The dialysis bag was boiled in 10% acetic acid and rinsed with distilled water. Rat plasma (2.1 ml) was added into a new clean dialysis bag equilibrated in PBS. A liposomal suspension (100 μl) containing 0.2 μCi of [^{3}H]MTX as tracer was added. The dialysis bag was secured with two knots at both ends to minimize air spaces as much as possible. The contents were mixed by squeezing gently and inverting the bag several times. The bag was rinsed with water and wiped carefully to dryness after tieing both ends to ensure that no traces of [^{3}H]MTX remained outside the bag. The bag was placed into 100 ml of PBS dialysate at 37°C with stirring at a speed of 50 opm (oscillation per min). 0.5-ml samples from 100 ml of dialysate were collected at the designated times and [^{3}H]MTX radioactivity was determined.

2.5. Animal studies

Male Wistar albino rats weighing 230–260 g were purchased from the Experimental Animal Breeding Center of Seoul National University (Seoul, South Korea). The rats were housed under laboratory conditions for 4 weeks and given food (Cheil Food and Chemical Co., I-cheon, South Korea) and water ad libitum. After anesthetization with urethane (1.125 g/kg, i.p.), the carotid artery and jugular vein were cannulated with a 23 gauge polyethylene cannula. About 0.2 ml of heparinized normal saline (100 U/ml) was used for flushing the cannula to prevent blood clotting. The free [^{3}H]MTX and liposome-entrapped [^{3}H]MTX equivalent to 200 μg per kg body weight of MTX and 5 μCi of [^{3}H]MTX as a tracer were intravenously administered via the jugular vein. Approx. 0.23 ml of blood samples were collected via the carotid artery at 0, 1, 3, 5, 10, 15, 20, 30, 60 and 120 min after drug administration and centrifuged immediately to minimize the potential blood storage effect. 100 μl of

plasma were pipetted for the determination of radioactivity.

Tissue distribution studies were performed as follows. At 15 and 120 min after i.v. injection of free [^{3}H]MTX and liposome-entrapped [^{3}H]-MTX, animals were killed. After blood was collected, liver, spleen, kidney, lung, heart, right (RLN) and left (LLN) ipsilateral iliac lymph nodes were immediately removed. The blood remaining in each organ was further removed by rinsing the organ with saline solution and blotted dry with the filter paper. Total weights of each organ were measured and approx. 0.1–0.2 g of tissue slices was excised for the determination of radioactivity.

2.6. Chromatographic separation of rat plasma

At 15 and 120 min after i.v. administration of the same doses of free [^{3}H]MTX and liposome-entrapped [^{3}H]MTX, 200 μl of plasma were applied to the 16×0.8 cm Sephadex G-50 (fine) column and eluted with PBS at a flow rate of approx. 0.2 ml/min. 1.5 ml of each fraction were collected for the determination of [^{3}H]MTX radioactivity.

2.7. Analysis of radioactivity

Samples were solubilized using 1 ml of Soluene-350® and the mixtures were heated at 50°C for 24 h followed by cooling to room temperature. Isopropyl alcohol (0.1 ml) and 30% of hydrogen peroxide (0.2 ml) were treated to decolorize highly colored samples such as liver and spleen. All samples treated with Soluene-350® were neutralized with 0.1 ml of 5 N HCl. 10 ml of scintillation cocktail consisting of POPOP (0.1 g) and PPO (5.5 g) in a mixture of toluene (667 ml) and Triton X-100 (333 ml) were then added and equilibrated for at least 24 h prior to radioactivity counting using a liquid scintillation counter. Total radioactivity was corrected to dpm (disintegrations per min) using the standard channel ratio quenching correction method. It should be noted that the total radioactivity measured represents not only [^{3}H]MTX but also the sum of all radioactivities of [^{3}H]MTX, liposome-entrapped [^{3}H]MTX and their possible metabolites.

2.8. Pharmacokinetic analysis

The noncompartmental pharmacokinetic parameters including the area under curve of the drug concentration-time (AUC) and area under moment curve (AUMC) of free [^{3}H]MTX and liposome-entrapped [^{3}H]MTX from zero to infinity were calculated by extrapolation according to the trapezoidal rule (Gibaldi and Perrier, 1982). The apparent elimination rate constant (λ) was directly calculated at the terminal slope by the linear least-squares method. The following standard methods were also used to calculate mean residence time (MRT), total clearance (Cl_t) and apparent volume of distribution at steady state (Vd_{ss}):

$$\mathrm{AUC} = \int_0^\infty C_p \, dt = \int_0^T C_p \, dt + \left[\frac{C_*}{\lambda}\right]$$

$$\mathrm{AUMC} = \int_0^\infty tC_p \, dt = \int_0^T tC_p \, dt + \left[\frac{TC_*}{\lambda}\right] + \left[\frac{C_*}{\lambda^2}\right].$$

$$\mathrm{MRT} = \mathrm{AUMC}/\mathrm{AUC}$$

$$t_{1/2} = 0.693/\lambda$$

$$Cl_t = \mathrm{dose}/\mathrm{AUC}$$

$$Vd_{ss} = \mathrm{MRT} \times Cl_t$$

where T and C_* indicate the last sampling time and concentration, respectively. C_p is the plasma concentration of MTX at time t.

2.9. Statistical analysis

The data were compared for statistical significance ($p < 0.05$) by the analysis of variance (ANOVA) test. All results were expressed as mean ± standard deviation (S.D.).

3. Results and discussion

3.1. In vitro release studies

The in vitro release of [^{3}H]MTX from liposomes in the presence of rat plasma was studied.

The release profiles of [^{3}H]MTX from liposomes as a function of incubation time are given in Fig. 1. The release profiles of [^{3}H]MTX from liposomes were almost the same shape, regardless of the surface charge. The release of [^{3}H]MTX from liposomes increased rapidly up to 4 h followed by much slower release over 8 h irrespective of the surface charge. However, the release profiles of drug from liposomes were dependent on the surface charge of liposomes. Negatively charged liposomes showed much greater [^{3}H]MTX release compared to positively charged and neutral liposomes. The amount of [^{3}H]MTX released from negatively charged, neutral and positively charged liposomes was 57, 36, and 22% at 2 h and 91, 54 and 49% at 8 h, respectively.

It is known that the release of drug entrapped into liposomes may be induced by the plasma constituents, cell surface proteins and lipoproteins possibly due to interaction of the liposomal surface with those factors (Allen and Cleland, 1980; Renswoude and Hoekstra, 1981; Kim et al., 1991). It was reported that the dianionic MTX and a positively charged amino acid could permeate through negatively charged liposomes more readily due to changes in elctrostatic repulsion between the positively charged choline in the lipid bilayer and drugs (Sada et al., 1990). The

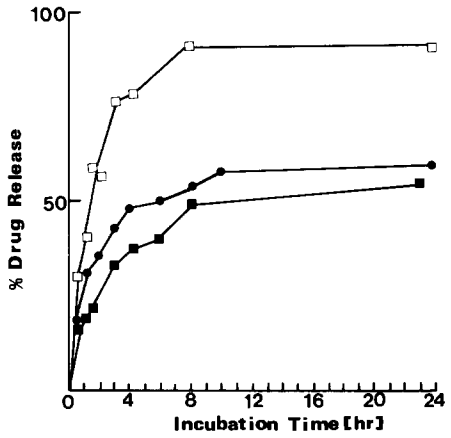

Fig. 1. In vitro release of [^{3}H]MTX from differently charged liposome-entrapped [^{3}H]MTX in the presence of rat plasma after incubation in PBS at 37°C at the rate of 50 opm. Negatively charged (□), neutral (●), and positively charged (■) liposomes.

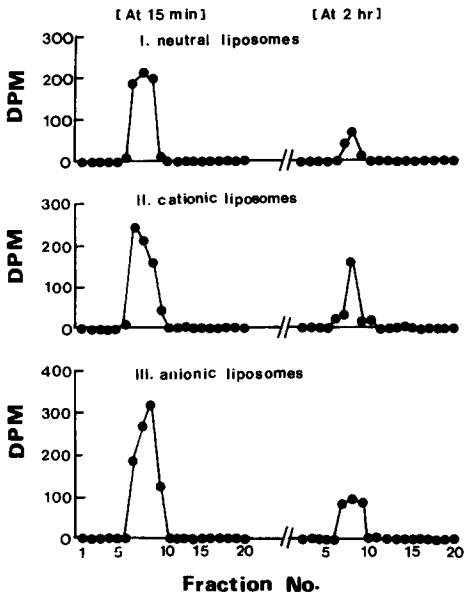

Fig. 2. Chromatographic separation of [^{3}H]MTX from rat plasma after i.v. administration of free [^{3}H]MTX and liposome-entrapped [^{3}H]MTX to rats.

enhanced in vitro release of [^{3}H]MTX from negatively charged liposomes in rat plasma may be due to the interaction of incorporated lipid compositions of liposomes with plasma components, resulting in a change in drug release through the lipid bilayers by destabilization of the liposomal membranes. The exact role of the surface charge of liposomes, drug and plasma components is not fully known. However, the drug release after uptake of liposomes in tissue as a target organ may be of significance in chemotherapy rather than drug release in plasma.

3.2. Chromatographic separation of rat plasma

The free and liposome-entrapped [^{3}H]MTX in rat plasma after i.v. injection were separated using a Sephadex G-50 gel column, showing how long liposome-entrapped [^{3}H]MTX could be maintained in blood. Fig. 2 shows that liposome-entrapped [^{3}H]MTX is eluted around fraction no. 5–11 and is present in blood up to 2 h. On the other hand, free [^{3}H]MTX was eluted at fraction no. 47–63 and was not clearly detected in eluent up to the 60-th fraction (data not shown) at 15

and 120 min after injection. The free [^{3}H]MTX concentration was very low in plasma due to rapid elimination and was scarcely detected by the chromatographic separation. [^{3}H]MTX in the blood circulation at 2 h is mainly present in the form of liposome-entrapped [^{3}H]MTX. While [^{3}H]MTX slowly released from charged liposomes in the plasma is rapidly eliminated from the circulatory system, a certain amount of liposome-entrapped [^{3}H]MTX was usually taken up by the specific tissues.

3.3. Pharmacokinetics of liposome-entrapped [^{3}H] MTX

The mean plasma concentration-time curves of [^{3}H]MTX after i.v. administration of free and liposome-entrapped [^{3}H]MTX to rats are given in Fig. 3. The elimination of [^{3}H]MTX from the blood stream showed biphasic patterns indicating rapid declining disposition up to 30 min followed by the slower elimination phase due to rapid tissue distribution and excretion through kidney. It was also reported that free [^{3}H]MTX showed rapid breakdown (> 97%) in plasma by the dihydrofolate reductase enzyme (Kimelberg et al., 1976; Kosloski et al., 1978). Liposome-entrapped [^{3}H]MTX maintained higher and longer plasma concentrations, and was mainly in the intact form in plasma compared to free [^{3}H]MTX for 2 h. It could be due to the body distribution of liposome-entrapped [^{3}H]MTX from blood circulation to macrophage-rich organs followed by slow release of [^{3}H]MTX from liposomes.

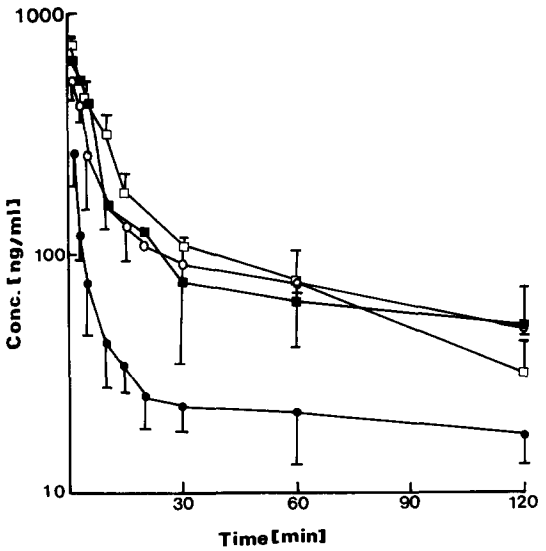

Fig. 3. Plasma concentration profiles of [^{3}H]MTX after i.v. administration of free [^{3}H]MTX and differently charged liposome-entrapped [^{3}H]MTX to rats. Free [^{3}H]MTX (●), negatively charged (□), neutral (○) and positively charged (■) liposomes.

The pharmacokinetic parameters of free [^{3}H]MTX and liposome-entrapped [^{3}H]MTX are listed in Table 1. Liposome-entrapped [^{3}H]MTX resulted in a higher AUC but lower Cl_t, and Vd_{ss} compared to free [^{3}H]MTX ($p < 0.01$). However, no statistically significance differences of AUC,

Table 1
Analysis of non-compartmental pharmacokinetic parameters of MTX after i.v. administration of free [^{3}H]MTX and liposome-entrapped [^{3}H]MTX to rats

Parameter	Free [^{3}H]MTX	Liposome-entrapped [^{3}H]MTX		
		Positively charged	Neutral	Negatively charged
AUC (μg min ml^{-1})	4.87 ± 1.86 [a]	17.9 ± 1.2 [c]	16.9 ± 4.3 [c]	16.9 ± 2.86 [c]
AUMC (μg min^2 ml^{-1})	624 ± 343	1880 ± 389 [c]	1666 ± 469 [c]	965 ± 223 [b]
MRT (min)	121.6 ± 28.0	106.1 ± 29.8	98.7 ± 6.2	56.4 ± 22.9 [c]
$t_{1/2}$ (min)	95.4 ± 25.3	97.5 ± 26.9	76.3 ± 11.1	55.7 ± 24.8 [b]
Cl_t (ml h^{-1} kg^{-1})	46.2 ± 17.9	11.2 ± 0.8 [c]	12.4 ± 3.0 [c]	12.0 ± 1.88 [c]
Vd_{ss} (ml kg^{-1})	5288 ± 1168	1201 ± 430 [c]	1220 ± 316 [c]	670 ± 284 [c]

[a] Mean ± S.D.($n \geq 3$).
[b] $p < 0.05$.
[c] $p < 0.01$ by the ANOVA test when compared to free [^{3}H]MTX. Note: The AUMC, MRT and $t_{1/2}$ of negatively charged liposome entrapped [^{3}H]MTX were significantly different when compared to positively charged liposomes ($p < 0.05$).

Table 2
Amounts (% dose/g tissue) of [^{3}H]MTX in various tissues at 15 min after i.v. administration of free [^{3}H]MTX and differently charged liposome-entrapped [^{3}H]MTX

Tissue	Free [^{3}H]MTX	Liposome-entrapped [^{3}H]MTX		
		Neutral	Positively charged	Negatively charged
Liver	2.71 ± 0.55 (37.1) [a]	2.03 ± 0.07 (8.79)	2.02 ± 0.34 (5.75)	1.90 ± 0.16 (5.59) [b]
Kidney	8.41 ± 0.31 (11.5)	6.84 ± 0.90 (29.6)	5.81 ± 2.48 (16.6) [b]	3.56 ± 0.70 (10.5) [c]
Spleen	0.24 ± 0.08 (3.29)	3.69 ± 1.02 (16.0) [c]	4.29 ± 0.77 (12.2) [c]	5.58 ± 1.32 (16.4) [c]
Lung	0.23 ± 0.01 (3.15)	1.33 ± 0.11 (5.76) [c]	0.69 ± 0.13 (1.97)	1.67 ± 0.10 (4.91) [c]
Heart	0.36 ± 0.08 (4.93)	0.27 ± 0.02 (1.17)	0.22 ± 0.05 (0.63)	1.20 ± 0.32 (3.53) [c]
RLN	0.61 ± 0.20 (8.36)	0.71 ± 0.43 (3.07)	0.87 ± 0.22 (2.48)	6.85 ± 2.83 (20.1) [c]
LLN	0.68 ± 0.28 (9.32)	0.30 ± 0.22 (1.30)	0.78 ± 0.37 (2.22)	2.82 ± 1.23 (8.29) [c]
Plasma	0.07 ± 0.01 (1.00)	0.23 ± 0.06 (1.00) [c]	0.35 ± 0.05 (1.00) [c]	0.34 ± 0.04 (1.00) [c]

Numbers in parentheses represent values of tissue-to-plasma (T/P) ratio.
[a] Mean ± S.D. ($n \geq 3$).
[b] $p < 0.05$.
[c] $p < 0.01$ by the ANOVA test when compared to free [^{3}H]MTX. Note: The difference between neutral and negatively charged liposomes was significant in spleen and lymph nodes (RLN, LLN) ($p < 0.05$).

Cl_t, and Vd_{ss} among differently charged liposomes were observed but the AUMC, MRT and $t_{1/2}$ of negatively charged liposome-entrapped drug were significantly different when compared to positively charged liposomes ($p < 0.05$). Negatively charged liposomes showed more rapid elimination in plasma compared to neutral and positively charged liposomes. These results were consistent with other works which reported rapid elimination of negatively charged liposomes (Juliano and Stamp, 1975; Senior et al., 1985; Tokunaga et al., 1988). The lower MRT and $t_{1/2}$ of negatively charged liposomes in plasma compared to free drug may have resulted from the rapid uptake by liver to a greater extent, possibly via the reticuloendothelial system (RES), since liposome-entrapped drug cannot be eliminated by kidney, the main eliminating organ for MTX (Spanjer et al., 1984). Liposome-entrapped [^{3}H] MTX enhanced bioavailability in plasma by retarding drug release, and protecting drug metabolism and clearance by lipid bilayers of liposomes. However, it should be noted that the radioactivity measured was the sum of radioactiv-

Table 3
Amounts (% dose/g tissue) of [^{3}H]MTX in various tissues at 120 min after i.v. administration of free [^{3}H]MTX and differently charged liposome-entrapped [^{3}H]MTX

Tissue	Free [^{3}H]MTX	Liposome-entrapped [^{3}H]MTX		
		Neutral	Positively charged	Negatively charged
Liver	2.21 ± 0.55 (35.6) [a]	2.46 ± 0.53 (15.2)	2.70 ± 0.36 (22.3)	5.34 ± 0.43 (51.3) [c]
Kidney	3.00 ± 2.29 (48.4)	7.47 ± 1.29 (46.1) [b]	3.48 ± 0.47 (28.8)	8.16 ± 1.38 (78.5) [b]
Spleen	0.093 ± 0.023 (1.50)	7.00 ± 0.72 (43.2) [c]	4.24 ± 0.52 (35.0) [b]	7.81 ± 1.75 (75.1) [c]
Lung	0.081 ± 0.034 (1.31)	0.97 ± 0.37 (5.99) [b]	0.52 ± 0.17 (4.30) [b]	2.94 ± 0.71 (28.3) [c]
Heart	0.086 ± 0.006 (1.39)	0.36 ± 0.03 (2.22)	0.31 ± 0.06 (2.56)	1.08 ± 0.62 (10.4) [b]
RLN	0.70 ± 0.09 (11.3)	2.93 ± 0.96 (18.1)	0.55 ± 0.13 (4.55)	6.11 ± 2.41 (58.8) [b]
LLN	0.87 ± 0.18 (14.0)	1.46 ± 0.76 (9.01)	0.87 ± 0.28 (7.19)	9.16 ± 2.78 (88.1) [b]
Plasma	0.062 ± 0.024 (1.00)	0.16 ± 0.05 (1.00) [b]	0.12 ± 0.04 (1.00)	0.10 ± 0.01 (1.00)

Numbers in parentheses represent values of tissue-to-plasma (T/P) ratio.
[a] Mean ± S.D. ($n \geq 3$).
[b] $p < 0.05$.
[c] $p < 0.01$ by the ANOVA test when compared to free [^{3}H]MTX. Note: The difference between positively charged and negatively charged liposomes was significant in liver, spleen, kidney, lung and lymph nodes (RLN, LLN) ($p < 0.05$).

ities of free and liposome-entrapped [^{3}H]MTX, and their possible metabolites.

3.4. Tissue distribution of liposome-entrapped [^{3}H]MTX

The tissue distribution of [^{3}H]MTX for each organ at 15 and 120 min after i.v. injection of free [^{3}H]MTX and liposome-entrapped [^{3}H]MTX is shown in Tables 2 and 3. [^{3}H]MTX was initially taken up to a considerable extent by the liver and kidney when compared to other tissues. The initial tissue-to-plasma ratio (T/P) was higher in liver and kidney. Liposome-entrapped [^{3}H]MTX gradually became more localized in liver, spleen, lung and lymph nodes compared to free [^{3}H]MTX ($p < 0.05$). There was markedly increased uptake of drug in spleen from negatively charged liposomes when compared to neutral and positively charged liposomes. While clearance of free drug in tissue was rapid, that of liposome-entrapped drug was slow from the tissues. It was noted that negatively charged liposomes led to greater localization of drug in liver, spleen, lung and lymph nodes at 2 h after i.v. injection compared to neutral and positively charged liposomes ($p < 0.05$). In addition, increased uptake of negatively charged liposomes in kidney and heart at 2 h was also observed, however, this needs to be validated later.

In accordance with our results, several investigators have reported that liposomes bearing negative surface charge accumulate in the lung to a greater extent than neutral and positively charged liposomes of similar size (Abra et al., 1984). As judged from the fact that negatively charged liposomes were highly localized in liver, spleen, lung and lymph nodes, negatively charged liposomes can be an effective vehicle for the delivery of anticancer agents to these sites. Although liposome-entrapped [^{3}H]MTX was widely distributed in tissues without the exact role of liposomal surface charge being known, it was obvious that the distribution of liposome-entrapped [^{3}H]MTX was significantly different when compared to free [^{3}H]MTX. Furthermore, the surface charge of liposomes altered the biodistribution of [^{3}H]MTX in rats.

In conclusion, the in vitro release rate of drug from negatively charged liposomes increased in the presence of rat plasma due to electrostatic interaction between positively charged choline and plasma constituents. The liposome-entrapped drug produced higher and longer plasma concentrations by retarding drug release, and protecting drug metabolism and clearance compared to free drug, but was rapidly taken up by the liver and other macrophage-rich organs after i.v. injection to rats. It was observed that negatively charged liposomes after i.v. injection to rats led to graeter localization in spleen, liver, lung and lymph nodes compared to neutral and positively charged liposomes. The elucidation of the effects of liposomal surface charge on the release and tissue disposition of drug are of significant value in view of selective delivery of liposome-entrapped anticaner drug to specific target tissues in chemotherapy and membrane biochemistry.

Acknowledgement

This research work was supported in part by a research grant from Korea Science and Engineering Foundation (KOSEF 901-0131-014-2) in 1990–1992.

References

Abra, R.M., Hunt, C.A. and Lau, D.T., Liposome distribution in vivo: VI. Delivery to the lung. *J. Pharm. Sci.*, 73 (1984) 203–206.

Allen, T.M. and Cleland, L.G., Serum induced leakage of liposome contents. *Biochim. Biophys. Acta*, 597 (1980) 418–426.

Bae, E.J., Lee, S.H., Lee, M.G., Hwang, S.J. and Kim, C.-K., Pharmacokinetics of methotrexate after intravenous and intramuscular injection of methotrexate-bearing neutral liposomes to rats. *J. Clin. Pharm. Ther.*, 18 (1993) 393–404.

Bleyer, W.A., The clinical pharmacology of methotrexate. *Cancer*, 41 (1978) 36–51.

Colley, C.M. and Ryman, B.E., Liposomes carriers in vivo for methotrexate. *Biochem. Soc. Trans.*, 3 (1975) 157–159.

Gibaldi, M. and Perrier, D., *Pharmacokinetics*, 2nd Edn, Revised and Expanded, Dekker, New York, 1982.

Hirano, K. and Hunt, C.A., Lymphatic transport of liposome-encapsulated agents: effects of liposome size following

intraperitoneal administration. *J. Pharm. Sci.*, 74 (1985) 915–921.

Jonah, M.M., Cerny, E.A. and Rahman, Y.E., Tissue distribution of EDTA encapsulated within liposomes of varing surface properties. *Biochim. Biophys. Acta*, 401 (1975) 336–348.

Juliano, R.L. and Stamp, D., The effect of particle size and charge on the clearance rates of liposomes and liposome encapsulated drugs. *Biochem. Biophys. Res. Commun.*, 63 (1975) 651–658.

Juliano, R.L., Stamp, D. and McCullough, N., Pharmacokinetics of liposome-entrapped anticancer drugs and implications for therapy. *Ann. NY Acad. Sci.*, (1978) 411–432.

Kim, C.-K., Choi, Y.-J., Lim, S.-J., Lee, M.G., Lee, S.-H. and Hwang, S.J., Lymph nodes targeting and pharmacokinetics of [^{3}H]methotrexate-encapsulated neutral large unilamellar vesicles and immunoliposomes. *Int. J. Pharm.*, 98 (1993a) 9–18.

Kim, C.-K., Kim, H.-S., Lee, B.-J. and Han, J.-H., Effect of bovine serum albumin on the stability of methotrexate-encapsulated liposomes. *Arch. Pharm. Res.*, 14 (1991) 336–341.

Kim, C.-K., Lee, S.-K. and Lee, B.-J., Preparation and evaluation of temperature sensitive liposomes containing adrimycin and cytarabine. *Arch. Pharm. Res.*, 16 (1993b) 129–133.

Kimelberg, H.K. and Atchison, M.L., Effects of entrapment in liposomes on the distribution, degradation and effectiveness of methotrexate in vivo. *Ann. NY Acad. Sci.*, (1978) 395–410.

Kimelberg, H.K., Tracy, T.F., Bibblecome, S.M., Jr and Bourke, R.S., The effect of entrapment in liposomes on the in vivo distribution of [^{3}H]methotrexate in a primate. *Can. Res.*, 36 (1976) 2949–2957.

Kirby, C., Clark, J. and Ggregoriadis, G., Effect of the cholesterol content of small unilamellar liposomes on their stability in vivo and in vitro. *Biochem. J.*, 186 (1980) 591–598.

Kosloski, M.J., Rosen, F., Milholland, R.J. and Papahadjopoulous, D., Effect of lipid vesicles (liposomes) encapsulation of methotrexate on its chemotherapeutic efficacy in solid rodent tumors. *Can. Res.*, 38 (1978) 2848–2853.

Mayhew, E., Lazo, R. and Vail, W.J., Preparation of liposomes entrapping cancer chemotherapeutic agents for experimental in vivo and in vitro studies. In Gregoriadis, G. (Ed.), *Liposome Technology,* CRC Press, Boca Raton, FL, Vol. II, 1984, pp. 23–24.

Rahman, Y.E., Hanson, W.R., Bharucha, J., Ainsworth, E.J. and Jaroslow, B.N., Mechanism of reduction of antitumor drug toxicity by liposome encapsulation. *Ann. NY Acd. Sci.*, (1978) 325–342.

Renswoude, J.V. and Hoekstra, D., Cell-induced leakage of liposome contents. *Biochemistry*, 20 (1981) 540–546.

Sada, E., Kato, S., Terashima, M. and Kawahara, H., Effects of surface charges and cholesterol content on amino acid permeabilities of small unilamellar vesicles. *J. Pharm. Sci.*, 79 (1990) 232–235.

Senior, J., Crawley, J.C.W. and Gregoriadis, G., Tissue distribution of liposomes exhibiting long half-lives in the circulation after intravenous injection. *Biochim. Biophys. Acta*, 839 (1985) 1–8.

Shen, D.D. and Azarnoff, D.L., Clinical Pharmacokinetics of methotrexate. *Clin. Pharmacokinet.*, 3 (1978) 1–13.

Spanjer, H.H., Morselt, H. and Scherphof, G.L., Lactosylceramide-induced stimulation of liposome uptake by Kuppfer cells. *Biochim. Biophys. Acta*, 774 (1984) 49–55.

Szoka, F., Jr and Papahadjopoulous, D., Procedure for preparation of liposomes with large internal aqueous space and high capture by reverse-phase evaporation. *Proc. Natl. Acad. Sci. USA*, 75 (1978) 4194–4198.

Tokunaga, Y., Iwasa, T., Fujisaki, J., Sawai, S. and Kagawama, A., Liposomal sustained release delivery system for intravenous injection: II. Design of liposome carriers and blood disposition of lipophilic mitomycin C prodrug-bearing liposomes. *Chem. Pharm. Bull.*, 36 (1988) 3557–3564.